BIOCHEMISTRY

ADP-ribose–derived nuclear ATP synthesis by NUDIX5 is required for chromatin remodeling

Roni H. G. Wright,[1,2] Antonios Lioutas,[1,2] Francois Le Dily,[1,2] Daniel Soronellas,[1,2] Andy Pohl,[1,2] Jaume Bonet,[2,3] A. S. Nacht,[1,2] Sara Samino,[4,5] Jofre Font-Mateu,[1,2] Guillermo P. Vicent,[1,2] Michael Wierer,[1,2]* Miriam A. Trabado,[6] Constanze Schelhorn,[7] Carlo Carolis,[6] Maria J. Macias,[7,8] Oscar Yanes,[4,5] Baldo Oliva,[2,3] Miguel Beato[1,2]†

Key nuclear processes in eukaryotes, including DNA replication, repair, and gene regulation, require extensive chromatin remodeling catalyzed by energy-consuming enzymes. It remains unclear how the ATP demands of such processes are met in response to rapid stimuli. We analyzed this question in the context of the massive gene regulation changes induced by progestins in breast cancer cells and found that ATP is generated in the cell nucleus via the hydrolysis of poly(ADP-ribose) to ADP-ribose. In the presence of pyrophosphate, ADP-ribose is used by the pyrophosphatase NUDIX5 to generate nuclear ATP. The nuclear source of ATP is essential for hormone-induced chromatin remodeling, transcriptional regulation, and cell proliferation.

The nucleus of human cells requires a substantial amount of energy to replicate or to repair the genome and to reprogram gene expression in response to external cues, ensuring genome accessibility to mediate the extensive changes in chromatin and nucleosome organization (*1*). The assumption is that nuclear energetic demands are met by adenosine triphosphate (ATP) from the mitochondria. Although this may be the case in steady-state situations, it may not be sufficient for sudden extensive changes in cromatin, and nearly 60 years ago it was proposed that ATP could be generated in isolated nuclei (*2*, *3*).

To address this issue, we measured ATP levels in living breast cancer cells by means of ATP/ADP ratio detectors targeted to the cell nucleus, mitochondria, or cytosol (*4*) (fig. S1, A to D). Progestin (R5020) exposure induced an increase of this ratio in some cell nuclei (Fig. 1A and fig. S1, E and F), a behavior that was not observed in cells exposed to solvent (EtOH) (Fig. 1B, right panel, and fig. S1G). Cells showing increased nuclear ATP also exhibited activated progesterone receptor (phospho-PR), whereas those with unchanged nuclear ATP levels were not hormone-responsive (Fig. 1C).

[1]Centre de Regulació Genòmica (CRG), Barcelona Institute for Science and Technology, Barcelona E-09003, Spain. [2]Universitat Pompeu Fabra, Barcelona E-08003, Spain. [3]Structural Bioinformatics Laboratory, Universitat Pompeu Fabra, Barcelona E-08003, Spain. [4]Metabolomics Platform, Spanish Biomedical Research Centre in Diabetes and Associated Metabolic Disorders (CIBERDEM), 28029 Madrid, Spain. [5]Center for Omic Sciences and Department of Electronic Engineering, Rovira i Virgili University, 43007 Tarragona, Spain. [6]Biomolecular Screening and Protein Technologies Unit, Centre de Regulació Genòmica, Barcelona E-08003, Spain. [7]Institute for Research in Biomedicine (IRB Barcelona), Barcelona Institute of Science and Technology, Barcelona 08028, Spain. [8]Catalan Institution for Research and Advanced Studies (ICREA), Barcelona, Spain.
*Present address: Max-Planck-Institut für Biochemie, Munich, Germany. †Corresponding author. Email: miguel.beato@crg.eu

Increased nuclear ATP was confirmed in the cell population by means of luciferase constructs (*5*) (fig. S1, H to J) and was compromised by inhibiting mitochondrial ATP production (Fig. 1D and fig. S1K), but not by inhibiting glycolysis with 2-deoxy-D-glucose (2DG) or 3-(3-pyridinyl)-1-(4-pyridinyl)-2-propen-1-one (3PO) (fig. S1, L to O). In response to glucose, diffusion of mitochondrial ATP led to an increase in nuclear ATP (fig. S1P). This increase could be inhibited by oligomycin (fig. S1Q), leading to rapid depletion of nuclear ATP; such a result indicates that the nucleus contains a finite pool of ATP. However, in cells exposed to hormone, nuclear ATP continued to increase even when mitochondrial ATP production was inhibited by oligomycin 10 min after hormone addition (fig. S1R). Thus, mitochondrial ATP is required only during the initial minutes of hormone response.

Progestin leads to global changes in gene expression and chromatin remodeling in T47D breast cancer cells, a process that is dependent on a transient increase of PARP1-mediated poly (ADP-ribose) (PAR) (*6*–*10*) (Fig. 2A). PARP1 inhibition prevented the accumulation of PAR, whereas inhibition of PAR glycohydrolase (PARG) resulted in its persistence (Fig. 2, A and B, and fig. S2, A and B). The concomitant transient decrease in cellular nicotinamide adenine dinucleotide (NAD^+) could be blocked by PARP inhibition (Fig. 2C). Both PAR and NAD^+ levels eventually returned to the basal state in a PARG-dependent process (Fig. 2, B and C). Hormone-induced nuclear ATP increase was dependent on PARP1 and PARG (Fig. 2, D and E, and fig. S2, C to F); no significant changes in mitochondrial or cytoplasmic ATP levels were observed (fig. S2, C to E). Specific siRNA (small interfering RNA) knockdown showed that this nuclear ATP is dependent on PARP1 and not on other PARP family members (fig. S2G). Thus, both the formation of PAR and its degradation to ADP-ribose (ADPR) are required for the increase in nuclear ATP levels.

PARP1 activity depends on the nuclear NAD synthase NMNAT1, which uses ATP from mitochondria (*11*). NMNAT1 depletion blocked the increase in nuclear ATP (Fig. 2, E and F, and fig. S2, H and I), explaining the inhibitory effect of oligomycin before but not after hormone exposure (Fig. 1D and fig. S1N). We hypothesize that after ~10 min of hormone exposure, sufficient NAD^+ has been accumulated (Fig. 2B) to sustain the generation of ADPR and nuclear ATP.

Proteomic analysis of material immunoprecipitated with a PAR antibody in control cells and cells exposed to hormone (Fig. 3A and fig. S3A) revealed 1091 poly-ADP-ribosylated or PAR-binding proteins (table S2). We focused on hormone-induced proteins involved in ADP and ADPR metabolism and identified the ADP-sugar pyrophosphatase NUDIX5 (also known as NUDT5) (*12*). Because NUDIX5 interacts with both PAR and PARG (fig. S3B), is overexpressed in breast cancer (fig. S3, C to F), and is the most abundant NUDIX family member in T47D cells (fig. S3G), we explored its involvement in nuclear ATP generation. NUDIX5 depletion (Fig. 3B) did not affect the mRNA levels of other NUDIX family members (fig. S3H) but markedly reduced the hormonal increase in nuclear ATP without affecting mitochondrial or cytoplasmic ATP (Fig. 3B and fig. S3I).

After incubation of recombinant NUDIX5 (fig. S4A) with ADPR and pyrophosphate (PPi), we detected the production of AMP and ATP both directly by mass spectrometry (Fig. 3C) and indirectly (fig. S4, B and C). In the absence of PPi, ATP generation with wild-type NUDIX5 and the catalytically inactive NUDIX5 mutant (EQ112) was comparable (fig. S4C). PPi partially decreased the efficiency of the canonical hydrolytic reaction generating AMP (fig. S4D). We observed ATP generation by NUDIX5 starting from labeled PAR in vitro, a reaction dependent on PARG and PPi (Fig. 3D and fig. S4, E and F). ATP synthesis is endergonic under standard conditions (ΔG_m = 12.3 ± 7.3 kJ/mol) (fig. S4G), and synthesis of AMP (ΔG_m = −22.2 ± 7.3 kJ/mol) is prevailing. Therefore, we hypothesize that ATP synthesis may result from increased concentrations of ADPR and PPi and possibly from posttranslational modifications of NUDIX5.

NUDIX5 is a homodimer (*13*). Phosphoproteomic analysis showed that NUDIX5 is phosphorylated at Thr^{45} (T45) before hormone treatment (fig. S5A). A NUDIX5 phospho-T45–specific antibody showed a decrease in phosphoNUDIX5 after hormone treatment (Fig. 3E). T45 phosphorylation is important for homodimer stability, and dephosphorylation resulted in its destabilization (Fig. 3, E and G, and movies S1 and S2), eventually facilitating ATP synthesis. Overexpressed NUDIX5 T45 phosphomimetic mutant (T45D) behaved as dominant negative for hormone-induced cell proliferation and gene regulation (Fig. 3H and fig. S5B). Relative to both wild-type NUDIX5 and the phospho-null mutant

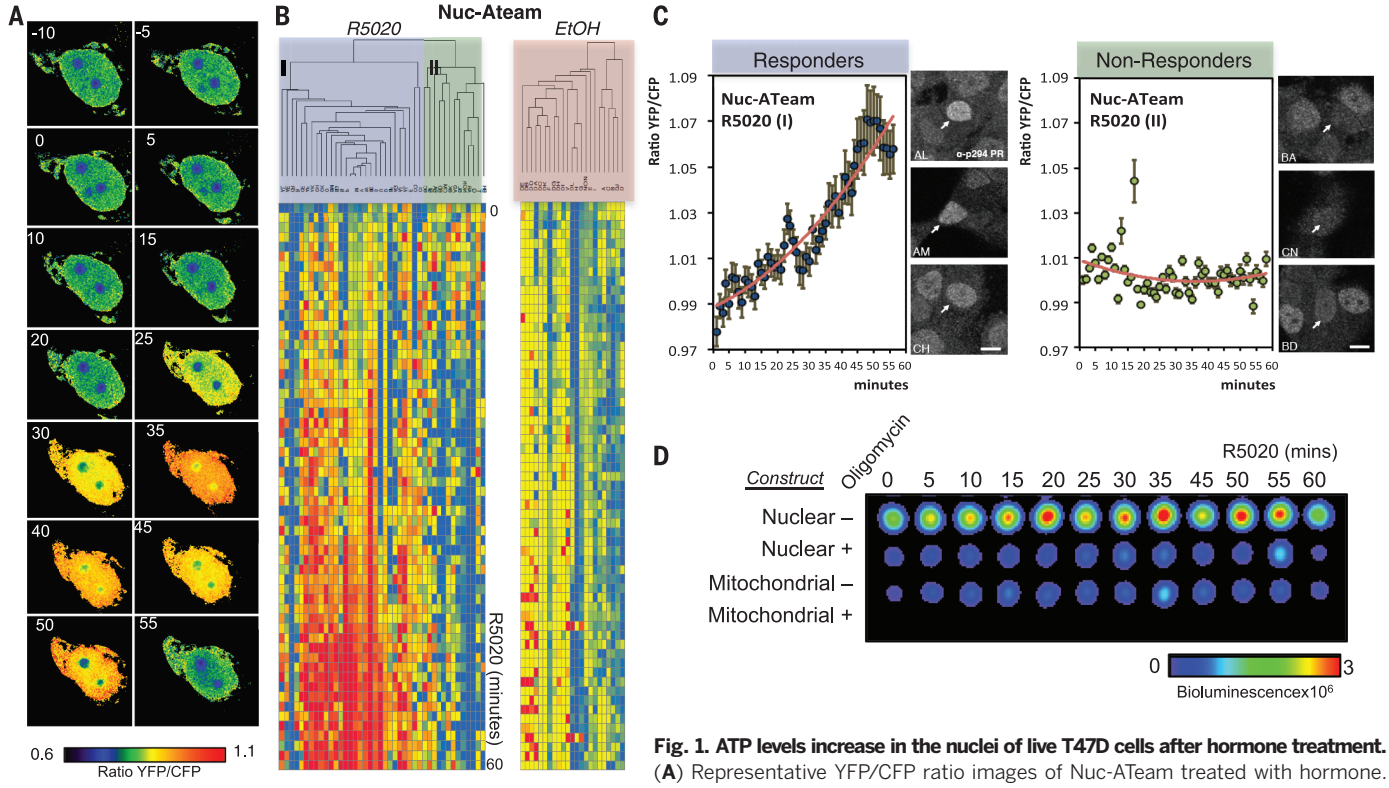

Fig. 1. ATP levels increase in the nuclei of live T47D cells after hormone treatment. (**A**) Representative YFP/CFP ratio images of Nuc-ATeam treated with hormone. (**B**) Hierarchical clustering of YFP/CFP average ratio from nuclei treated with hormone (left) or solvent (EtOH) (right). (**C**) Quantification of data presented in (B). Cluster I "responders" show increases in both nuclear ATP and phospho-PR S294; cluster II "nonresponders" show no increase in nuclear ATP or phospho-PR S294. Scale bar, 10 μm; arrows indicate the cells imaged. (**D**) Bioluminescence image of T47D cells treated with progestin, with (+) or without (–) prior oligomycin treatment.

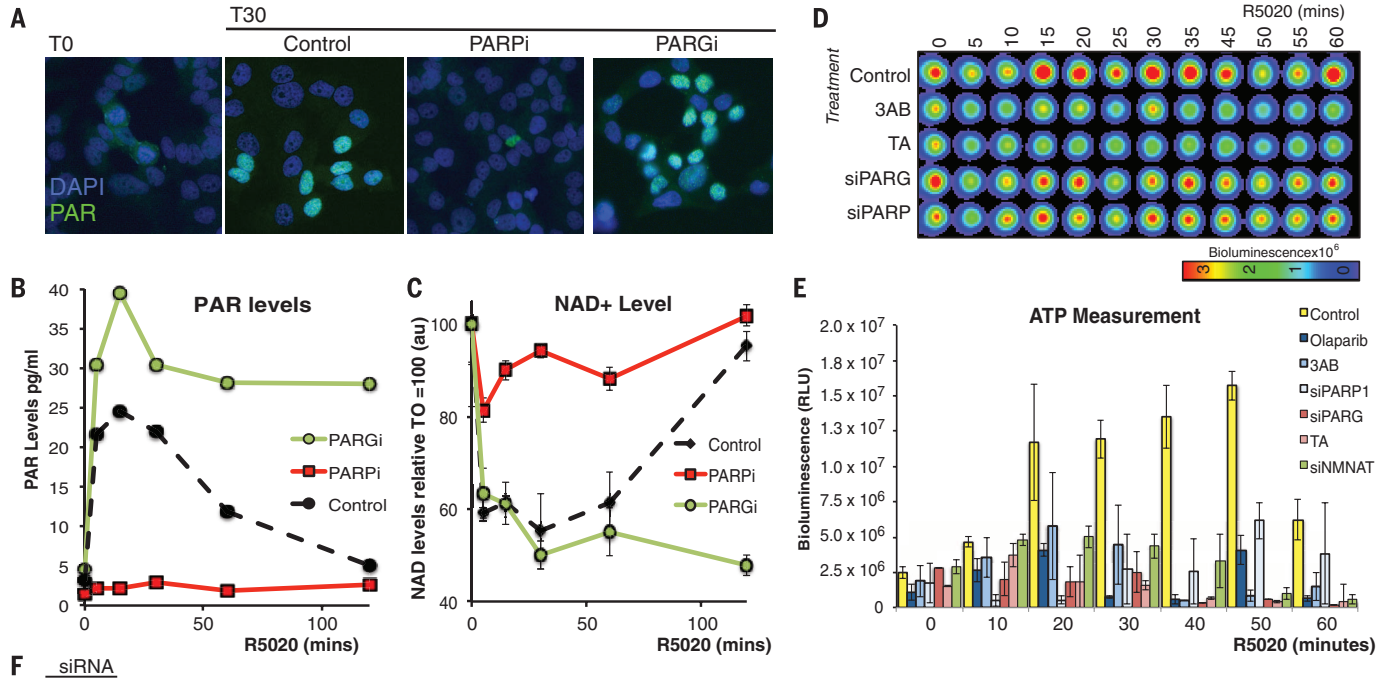

Fig. 2. Effect of PAR synthesis and degradation on the hormonal increase in nuclear ATP levels. (**A** and **B**) PAR levels after hormone treatment for 30 min, measured by immunofluorescence (A) or enzyme-linked immunosorbent assay (B) in the absence (control) or presence of PARP inhibitors (PARPi) or PARG inhibitors (PARGi). DAPI, 4′,6-diamidino-2-phenylindole. (**C**) NAD^+ levels in cells exposed to hormone alone (control) or in the presence of PARPi or PARGi (mean ± SEM). (**D**) Representative bioluminescence image of nuclear ATP levels in the absence (control) or presence of PARPi (3AB) or PARGi (TA) or knockdown of PARP1 (siPARP1) or PARG (siPARG). (**E**) Quantification (mean ± SEM) of ATP measurements after PARP1 (olaparib, 3AB, siPARP1), PARG (TA, siPARG), and NMNAT1 inhibition. (**F**) Knockdown of NMNAT1 quantified by Western blot.

T45A-NUDIX5, phospho-mimetic T45D-NUDIX5 strongly resisted conformational changes (fig. S5, C and D). Moreover, both wild-type and T45A-NUDIX5 (fig. S4A) generated ATP in the presence of PPi, whereas T45D-NUDIX5 did not (fig. S5E). In contrast, AMP generation by T45 mutants was only slightly affected by PPi (fig. S5, F to J; K_d values: wild type, 3.90 ± 0.41 μM; T45A, 4.44 ± 0.53 μM; T45D, 1.84 ± 1.07 mM).

We next explored the requirement of nuclear ATP for gene regulation. PARG inhibition or NUDIX5 depletion compromised regulation of 50% of hormone-responsive genes, with a clear overlap (Fig. 4A). The majority (70%) of NUDIX5- and PARG-dependent genes required both activities, and most of these genes also depended on poly-ADP-ribosylation (Fig. 4B). Progestin-induced cell proliferation is abrogated by inhibition of PAR formation (*9*) and by depletion of PARG or NUDIX5 (Fig. 4C). Estrogen-induced MCF7 breast cancer cells showed increases in PAR and nuclear ATP that were dependent on the activities of PARP, PARG, and NUDIX5 (fig. S5, A to D). Gene expression changes and cell proliferation in response to estrogen were also dependent on these enzymes (Fig. 4, C and D).

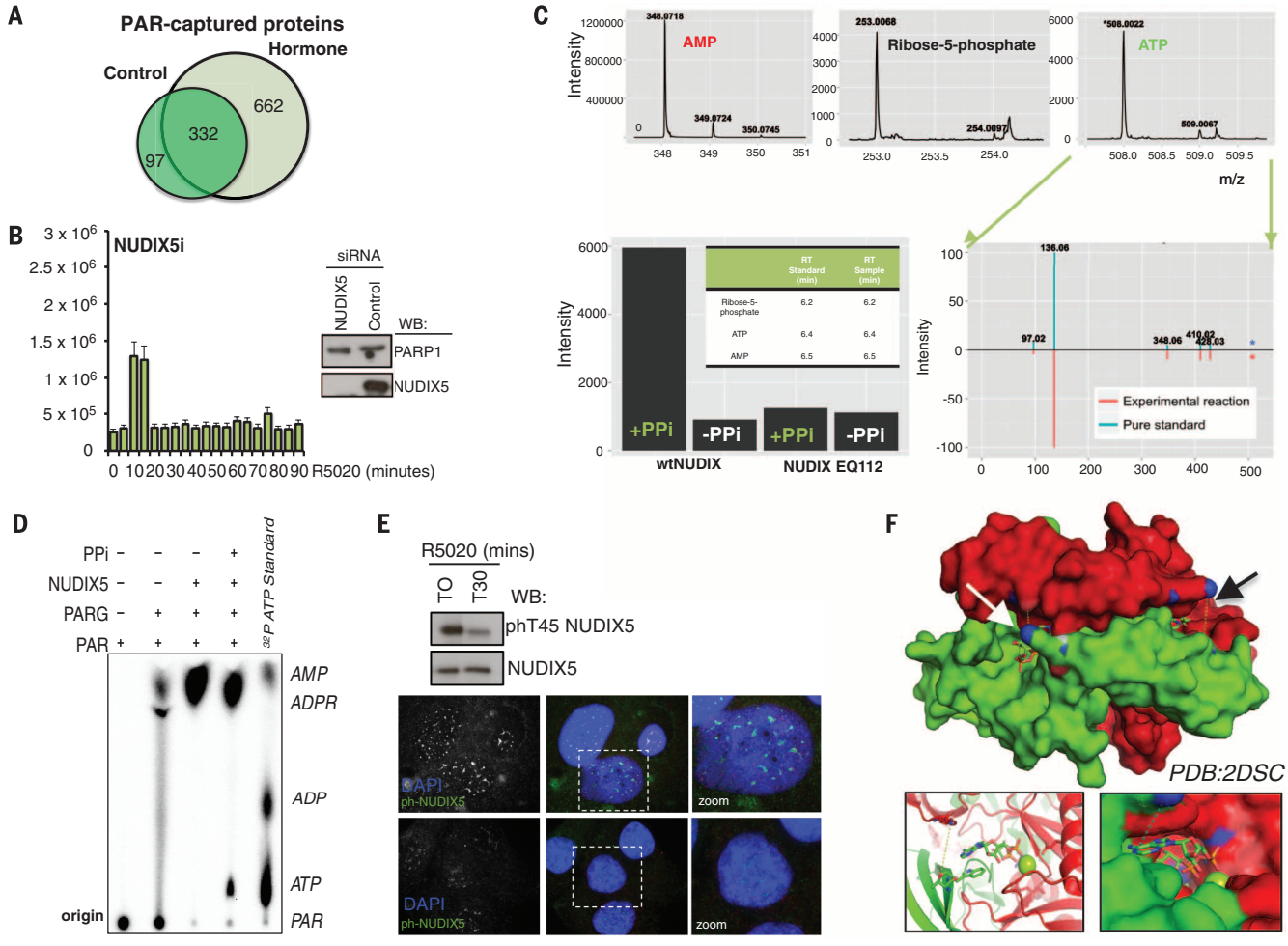

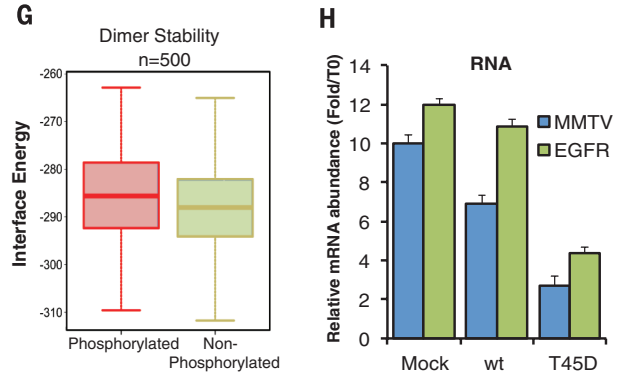

Fig. 3. Role of NUDIX5 in ATP synthesis in cell nuclei and in vitro. (**A**) Proteins captured by an antibody to PAR and identified by mass spectrometry. (**B**) Left: Quantification (mean ± SEM) of nuclear ATP by bioluminescence in cells depleted of NUDIX5 (NUDIX5i). Right: Protein levels measured by Western blot. (**C**) Relative ATP levels measured by high-resolution mass spectrometry using either wild-type or catalytically inactive NUDIX5 (EQ112) and ADPR in the presence or absence of PPi. Inset table: Retention time (RT) of AMP, ribose-5-phosphate, and ATP standards using hydrophilic interaction liquid chromatography (HILIC). (**D**) Production of ATP via ADPR derived from the hydrolysis of PAR by PARG, as visualized by thin-layer chromatography and autoradiography. (**E**) Phospho-T45 NUDIX5 in T47D^{wt} cells measured by Western blot (top) or immunofluorescence (bottom). (**F**) Crystal structure of NUDIX5 homodimer complex with ADPR and Mg^{2+} (PDB: 2DSC). Top: Two symmetrical contacts between T45D (blue) and K27 from the complementary chains are indicated (arrows). Bottom: View of active site of T45D with ADPR and Mg^{2+} (green sphere). (**G**) Dimer stability/interface energies calculated by MODELLER between 500 decoys of NUDIX5, nonphosphorylated (left) or phosphorylated (right) Wilcoxon (2.2×10^{-4}), and *t* distributions (4.14×10^{-4}). (**H**) T45D-NUDIX5 mutant behaves as dominant negative upon progesterone-induced gene expression; values are means ± SEM.

In response to progestin, initial displacement of histone H1 or H2A is dependent on PARP1 activity (*10*) but independent of PARG or NUDIX5, whereas later displacement depends on all three activities (fig. S6, E and F). Thus, initial nucleosome remodeling uses an already existing pool of nuclear ATP (Fig. 1), whereas the subsequent remodeling steps depend on PAR-derived nuclear ATP. The extent of global chromatin remodeling (H1, H2A) and recruitment of PARP1 and the ATPase bromodomain PHD finger transcription factor (BPTF) correlates well with the need for nuclear ATP (Fig. 4, E to G), which is required for extensive ATP-dependent chromatin remodeling.

In breast cancer cells, PR interacts with PARP1 (*10*) and with the DNA-dependent protein kinase Ku (*14*), which suggests that PAR and ATP could be involved in DNA repair (*15*–*17*). Indeed, survival of MCF7 cells after DNA damage is dependent on PARP1, PARG, and NUDIX5 (fig. S7, A and B). There is evidence that hormone-induced gene expression changes, and the torsional stress endured by the chromatin is relieved by local DNA cleavage (*18*). After damage, PAR could serve as a local source of ATP for the extensive chromatin remodeling associated with the repair process.

Recently it was shown that PAR acts as a "seed" during nuclear compartmentalization by liquid demixing (*19*); such transient molecular sieves mediated by intrinsically disordered proteins may also provide a local favorable environment for ATP generation by NUDIX5. These so-called "membraneless" organelles may serve to concentrate not only the enzymes but also the substrates required for ATP generation, leading to a local increase and specific environment for chromatin remodeling and/or repair.

Our work describes a mechanism for energy generation in the nuclei of breast cancer cells exposed to hormone. The high energetic cost of global chromatin modification is covered via the conversion of ADPR to ATP and ribose-5-phosphate catalyzed by the dephosphorylated form of NUDIX5. The pathway is ignited by mitochondrial ATP required for NMNAT1-mediated synthesis of NAD^+, which is converted to PAR by activated PARP1 and hydrolyzed to ADPR by PARG (fig. S7, C and D). Nuclear ATP levels increase after hormone exposure independently of ongoing mitochondrial and cytoplasmic ATP sources but dependent on nuclear ADPR and PPi. This nuclear ATP is required for chromatin remodeling, transcriptional regulation, and ultimately cell proliferation.

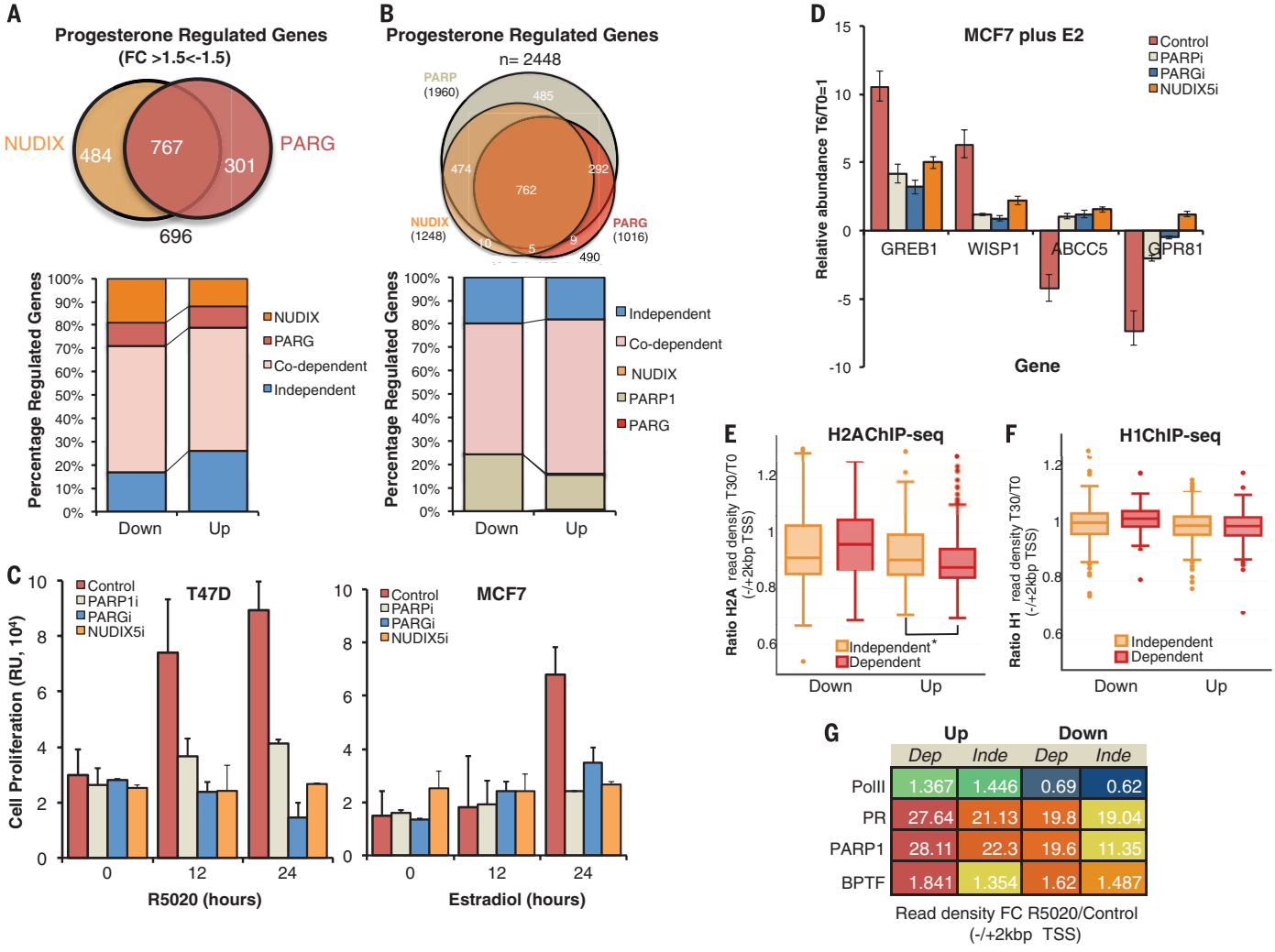

Fig. 4. ADPR-derived ATP is essential for hormone-induced gene expression and chromatin remodeling. (**A** and **B**) Top: Overlap of progesterone-regulated genes [fold change (FC) > 1.5 or FC < –1.5, $P < 0.05$]. Bottom: Quantification of up and down progesterone-regulated genes dependent on PARG and/or NUDIX (A) or PARP, PARG, and/or NUDIX (B). (**C**) Hormone-induced cell proliferation in T47D (left) or MCF7 (right) cells in the absence (control) or presence of PARPi or PARGi, or after knockdown of NUDIX5 (NUDIX5i); values are means ± SEM. (**D**) Estrogen (E2) target gene (GREB1, WISP1, ABCC5, GPR81) expression in the absence (control) or presence of PARPi or PARGi or after NUDIX5 depletion; values are means ± SEM. (**E** and **F**) Global analysis of H2A (E) and H1 (F) displacement as assessed by chromatin immunoprecipitation sequencing; *$P = 0.018$. (**G**) Recruitment of RNA polymerase II (Pol II), PR, PARP1, or BPTF to promoters of progesterone target genes, dependent (dep) or independent (inde) of NUDIX5 activity.

NUDIX5 overexpression in cancer patients correlates with a poor outcome in several cancer types, including breast cancer (fig. S8, A and B). The correlation with high expression of PARP1 (fig. S8C) may suggest that cancer cells depend on nuclear ATP generation. Hence, NUDIX5 is a promising target for PARP1 combinatorial drug therapy (*20*).

REFERENCES AND NOTES

1. G. J. Narlikar, M. L. Phelan, R. E. Kingston, *Mol. Cell* **8**, 1219–1230 (2001).
2. V. G. Allfrey, A. E. Mirsky, *Proc. Natl. Acad. Sci. U.S.A.* **43**, 589–598 (1957).
3. I. Betel, *Arch. Biochem. Biophys.* **134**, 271–274 (1969).
4. H. Imamura *et al.*, *Proc. Natl. Acad. Sci. U.S.A.* **106**, 15651–15656 (2009).
5. J. Hageman, M. J. Vos, M. A. van Waarde, H. H. Kampinga, *J. Biol. Chem.* **282**, 34334–34345 (2007).
6. G. P. Vicent *et al.*, *PLOS Genet.* **5**, e1000567 (2009).
7. G. P. Vicent *et al.*, *Genes Dev.* **25**, 845–862 (2011).
8. C. Ballaré *et al.*, *Mol. Cell* **49**, 67–79 (2013).
9. F. Le Dily *et al.*, *Genes Dev.* **28**, 2151–2162 (2014).
10. R. H. G. Wright *et al.*, *Genes Dev.* **26**, 1972–1983 (2012).
11. T. Zhang *et al.*, *J. Biol. Chem.* **287**, 12405–12416 (2012).
12. A. G. McLennan, *Cell. Mol. Life Sci.* **63**, 123–143 (2006).
13. M. Zha, C. Zhong, Y. Peng, H. Hu, J. Ding, *J. Mol. Biol.* **364**, 1021–1033 (2006).
14. C. A. Sartorius, G. S. Takimoto, J. K. Richer, L. Tung, K. B. Horwitz, *J. Mol. Endocrinol.* **24**, 165–182 (2000).
15. H. Maruta, N. Matsumura, S. Tanuma, *Biochem. Biophys. Res. Commun.* **236**, 265–269 (1997).
16. S. L. Oei, M. Ziegler, *J. Biol. Chem.* **275**, 23234–23239 (2000).
17. H. Maruta *et al.*, *Biol. Pharm. Bull.* **30**, 447–450 (2007).
18. B. G. Ju *et al.*, *Science* **312**, 1798–1802 (2006).
19. M. Altmeyer *et al.*, *Nat. Commun.* **6**, 8088 (2015).
20. K. M. Frizzell, W. L. Kraus, *Breast Cancer Res.* **11**, 111 (2009).

ACKNOWLEDGMENTS

We thank H. Kampinga for the luciferase plasmids, H. Imamura for the Ateam plasmids, M. Jacobson for the PARG-GST plasmid, V. Schreiber for the PARP1-GST plasmid, S. Capdevila and J. M. Caballero for support with IVIS, and J. Valcarcel for advice with the manuscript and CRG core facilities. Supported by the Spanish MEC (CSD2006-00049; BMC 2003-02902 and 2010-15313), and Catalan government (AGAUR) grants BIO2014-57518-R (B.O.), SAF2011-30578 (O.Y.), and BFU2014-53787-P (M.J.M.). CRG and IRB Barcelona are recipients of the Severo Ochoa Award of Excellence from MINECO (Spain). Global data sets have been deposited in GEO with accession numbers GSE53855, GSE64136, GSE64161, and GSE64163.

SUPPLEMENTARY MATERIALS

www.sciencemag.org/content/352/6290/1221/suppl/DC1
Materials and Methods
Supplementary Text
Figs. S1 to S8
Tables S1 to S8
Movies S1 and S2
References (*21*, *22*)

24 November 2015; accepted 9 May 2016
10.1126/science.aad9335

RNA TRANSCRIPTION

TT-seq maps the human transient transcriptome

Björn Schwalb,[1]* Margaux Michel,[1]* Benedikt Zacher,[2]* Katja Frühauf,[3] Carina Demel,[1] Achim Tresch,[4,5] Julien Gagneur,[2]†‡ Patrick Cramer[1,3]‡

Pervasive transcription of the genome produces both stable and transient RNAs. We developed transient transcriptome sequencing (TT-seq), a protocol that uniformly maps the entire range of RNA-producing units and estimates rates of RNA synthesis and degradation. Application of TT-seq to human K562 cells recovers stable messenger RNAs and long intergenic noncoding RNAs and additionally maps transient enhancer, antisense, and promoter-associated RNAs. TT-seq analysis shows that enhancer RNAs are short-lived and lack U1 motifs and secondary structure. TT-seq also maps transient RNA downstream of polyadenylation sites and uncovers sites of transcription termination; we found, on average, four transcription termination sites, distributed in a window with a median width of ~3300 base pairs. Termination sites coincide with a DNA motif associated with pausing of RNA polymerase before its release from the genome.

Transcription of eukaryotic genomes produces protein-coding mRNAs and diverse noncoding RNAs (ncRNAs), including enhancer RNAs (eRNAs) (*1*, *2*). Most ncRNAs are rapidly degraded, difficult to detect, and thus far have not been mappable in their full range. Mapping of transient RNAs is required, however, for analysis of RNA sequence, function, and fate.

We developed transient transcriptome sequencing (TT-seq), a protocol that maps transcriptionally active regions and enables estimation of RNA synthesis and degradation rates. TT-seq is based on 4sU-seq, which involves a brief exposure of cells to the nucleoside analog 4-thiouridine (4sU) (Fig. 1A) (*3*). 4sU is incorporated into RNA during transcription, and the resulting 4sU-labeled RNAs are isolated and sequenced. 4sU-seq is more sensitive than RNA-seq in detecting transient RNAs. However, 4sU-seq fails to map human transcripts uniformly, because only a short 3′ region of nascent transcripts is labeled during a 5-min exposure to 4sU, and the long preexisting 5′ regions dominate the sequencing data. To remove this 5′ bias, TT-seq uses RNA fragmentation before isolation of labeled RNA fragments (Fig. 1A). Thus, TT-seq measures only newly transcribed RNA fragments and provides the number of polymerases transcribing a genomic position within 5 min.

When applied to human K562 cells, TT-seq samples newly transcribed regions uniformly, whereas 4sU-seq produces a 5′ bias (fig. S1A). The coverage of short-lived introns with respect to exons is estimated (*4*) to be 60% for TT-seq, whereas it is 23 and 8% for 4sU-seq and RNA-seq, respectively (figs. S1A and S2). TT-seq is highly reproducible (fig. S3) and enables complete mapping of transcribed regions, complementing the GRO-cap (*5*) and CAGE (*6*) protocols, which detect RNA 5′ ends (Fig. 1B). TT-seq monitors RNA synthesis, whereas protocols such as PRO-seq (*7*), NET-seq (*8*), and mNET-seq (*9*) detect RNAs attached to polymerase. Therefore, the latter protocols yield peak signals near the promoter where polymerase pauses (Fig. 1B), whereas TT-seq does not. For paused and active genes (*10*), TT-seq reveals higher rates of RNA synthesis near the promoter relative to other regions (fig. S1B).

Using TT-seq data and the segmentation algorithm GenoSTAN (*4*, *11*), we identified 21,874 genomic intervals of apparently uninterrupted transcription (transcriptional units, TUs) (Fig. 2 and fig. S4A). TT-seq is highly sensitive, recovering 65% of transcription start sites (TSSs) obtained by GRO-cap (overlapping annotations within ± 400 bp) (*5*). A total of 8543 TUs overlapped GENCODE annotations (*12*) in the sense direction of transcription (50% reciprocal overlap of annotated regions; fig. S4B). This analysis detected 7810 mRNAs, 302 long intergenic noncoding RNAs (lincRNAs), and 431 antisense RNAs (asRNA). The 2916 TUs that shared less than 50% of their length with GENCODE annotations were not classified. The remaining 10,415 TUs (48%) represented newly detected ncRNAs that we characterized further.

Transcripts arise from promoters but also from enhancers, which are regulatory elements with characteristic chromatin modifications (*13*, *14*). To detect chromatin regions comprising putative enhancers and promoters (chromatin states), we applied GenoSTAN (*11*) to ENCODE ChIP-seq (chromatin immunoprecipitation–sequencing) data (*15*) for the coactivator p300 and a series of histone modifications (H3K27me3, H3K36me3, H4K20me1, H3K4me1, H3K4me3, H3K9ac, and

[1]Department of Molecular Biology, Max Planck Institute for Biophysical Chemistry, Am Faßberg 11, 37077 Göttingen, Germany. [2]Gene Center Munich, Ludwig-Maximilians-Universität München, Feodor-Lynen-Straße 25, 81377 Munich, Germany. [3]Department of Biosciences and Nutrition, Center for Innovative Medicine, and Science for Life Laboratory, Karolinska Institutet, Novum, Hälsovägen 7, 141 83 Huddinge, Sweden. [4]Department of Biology, University of Cologne, Zülpicher Straße 47, 50647 Cologne, Germany. [5]Max Planck Institute for Plant Breeding Research, Carl-von-Linné Weg 10, 50829 Cologne, Germany. *These authors contributed equally to this work. †Present address: Department of Informatics, Technische Universität München, Boltzmannstraße 3, 85748 Garching, Germany. **‡Corresponding author. Email: gagneur@in.tum.de (J.G.); patrick.cramer@mpibpc.mpg.de (P.C.)**